Journal of Advances in Mathematics and Computer Science

28(1): 1-20, 2018; Article no.JAMCS.42481
ISSN: 2456-9968
(Past name: British Journal of Mathematics & Computer Science, Past ISSN: 2231-0851)

Influence of Chemical Reaction, Viscous Dissipation and Joule Heating on MHD Maxwell Fluid Flow with Velocity and Thermal Slip over a Stretching Sheet

I. G. Baoku[1*]

[1]Department of Mathematical Sciences, Federal University, Dutsin-Ma, Katsina State, Nigeria.

Author's contribution

The sole author designed, analyzed, interpreted and prepared the manuscript.

Article Information

DOI: 10.9734/JAMCS/2018/42481
Editor(s):
(1) Dr. Mehmet Sirin Demir, Professor, Department of Mechanical Engineering, Faculty of Engineering, Istanbul University, Avcilar Campus 34320 Istanbul, Turkey.
Reviewers:
(1) Jawad Raza, Universiti Utara Malaysia, Malaysia.
(2) Imdat Taymaz, Sakarya University, Turkey.
Complete Peer review History: http://www.sciencedomain.org/review-history/25478

Original Research Article

Received: 1st June 2018
Accepted: 9th July 2018
Published: 11th July 2018

Abstract

A numerical integration scheme involving a fourth-fifth Runge-Kutta-Fehlberg method (RKF45) with shooting technique is employed to investigate a steady laminar incompressible forced convective flow of an upper-convected Maxwell fluid which is subjected to a transversely uniform magnetic field past a stretching sheet. Taking into account the velocity and thermal slip boundary conditions, the chemically reactive Maxwell fluid is examined in the presence of viscous dissipation and Joule heating. Using the similarity transformations, the momentum, energy and species concentration equations are transformed into a set of coupled nonlinear ordinary differential equations while the continuity equation is satisfied. The RKF45 solutions are obtained; verified with other results by homotopy analysis method that have been previously published in the literature and are found to be in good agreement. This close agreement supports the present analysis and accuracy of the numerical computations. The effects of the emerging flow parameters on the dimensionless velocity, temperature and species concentration distributions have been presented graphically and discussed. This article also includes a representative set of numerical results for local skin friction coefficient, Nusselt and Sherwood numbers in tables for various values of the governing parameters. It is concluded that the thermal boundary layer thickness is increased by increasing values of Hartmann number, Eckert number and thermal slip parameter while the local Nusselt and Sherwood numbers are enhanced by increments in the values of suction and stretching parameters.

Corresponding author: E-mail: ibaoku@fudutsinma.edu.ng;

Keywords: *Velocity slip; thermal slip; Maxwell fluid; magneto hydrodynamics; chemical reaction; viscous dissipation; Joule heating.*

1 Introduction

The study of laminar boundary layer flow and heat transfer analysis over a continuous moving or stretching surface has received considerable attentions due to its application in many polymer industries and several manufacturing processes such as paper production, wire drawing, glass-fiber, polymer extraction of plastic sheets, manufacturing of polymeric sheets, drawing of plastic films, etc. With the pioneering work of Crane [1], he examined the steady boundary layer flow of an incompressible viscous fluid over a linearly stretching plate and provided an exact similarity solution in closed analytical form. Crane's study was extended by many investigators such as Pavlov [2], Gupta and Gupta [3], Chen and Char [4] considering the effect of heat and mass transfer analysis alongside magnetic field under various physical conditions. Other authors [5-26] have discussed many aspects of linearly or nonlinearly stretching and other surfaces on viscous and non-Newtonian fluids and obtained similar analytical and/or numerical solutions.

There has been growing interest in the study of effects of viscous and Joule heating on the MHD flow and heat transfer due to their important roles in various devices which are subjected to large variations of gravitational force or which operate at high speeds. The applications of viscous dissipation and Ohmic heating on heat exchanger designs, wire and glass fiber drawing and on nuclear engineering in connection with the cooling of reactors cannot be overemphasized. El-Amin [27] studied the effects of both first- and second-order resistance, due to the solid matrix of non-Darcy porous medium, Joule heating and viscous dissipation on forced convection flow from a horizontal circular cylinder under the action of a transverse magnetic field. He considered the case of variable wall temperature conditions. Combined effects of Joule heating and viscous dissipation on the momentum and thermal transport were investigated for the magnetohydrodynamic (MHD) flow over a stretching sheet by Chen [28]. His results demonstrated that the reduction in heat transfer due to Joule and viscous heating was more pronounced at a higher Prandtl number while the Eckert number had an unimpressive effect on the velocity when the free convection was weak. Palani and Kim [29] performed a numerical investigation to study the MHD free convection flow past a semi-infinite inclined plate subjected to a variable surface temperature, taking into account Joule heating and viscous dissipation effects. They observed that the MHD parameter had retarding effects on velocity.

Recently, a numerical analysis was presented to study combined effects of viscous dissipation and Joule heating on MHD free-convective flow of a fluid with variable properties near a linearly stretching isothermal vertical sheet by Jaber [30]. Jaber [31] further numerically investigated the effects of Joule heating and viscous dissipation on MHD viscous fluid flow over a stretching porous horizontal sheet subjected to power law heat flux in the presence of heat source. An analysis was carried out to investigate the effects of suction and thermal radiation on the unsteady convective hydromagnetic flow and heat transfer in a third grade fluid in the presence of viscous dissipation and Joule heating effects over an infinite vertical plate by Baoku [32]. Solving the governing time-based coupled partial differential equations numerically by applying an efficient and unconditionally stable Crank-Nicolson finite difference scheme, he concluded that an increase in the suction parameter is observed to decrease the fluid velocity while the temperature distribution decreases with an increase in the thermal radiation parameter. Kumar et al. [33] examined combined effects of Joule heating and viscous dissipation on a three-dimensional flow of Oldroyd-B nanofluid. They gave a model that described the flow generated by bidirectional stretching sheet with thermophoresis and Brownian motion effects in the presence of radiation term. They concluded that combination of Joule and viscous heating increased the temperature of Oldroyd B nanofluid profile. Muhammad et al. [34] developed a three-dimensional stretched MHD flow of viscous fluid in the presence of prescribed heat flux(PHF), prescribed concentration flux(PCF), chemical reaction, viscous dissipation and Joule heating effects.

Literature is not sufficient on the slip flow, heat and mass transfer of non-Newtonian fluid. Flow patterns characterized by the slip boundary conditions have special significances in many scientific, industrial and technological applications. In some instances, the fluid presents a loss of adhesion at the wetted wall which compels it to slide along the wall. The concept of wall slip is crucial in describing the macroscopic effects of

certain molecular phenomena in the study of fluid-solid interaction problems. Consideration of no-slip condition seems unrealistic for many non-Newtonian flows because they exhibit macroscopic wall slip. Particularly, no-slip condition is inadequate for rough surface and in micro-electromechanical system (MEMS). The fluid exhibiting boundary slip finds applications in technology such as in the polishing of artificial heart and internal cavities in a variety of manufacturing parts is achieved by imbedding such fluid as abrasive Sajid et al. [35]. Other researchers who studied the non-Newtonian fluids subject to slip boundary conditions are in [36-46].

However, few works on the flow with slip conditions of Maxwell fluids over stretching sheets or surfaces are those of Hayat et al. [47], Vieru and Zafar [48], Sajid et al. [49] and Liu and Guo [50]. In all the aforementioned investigations, the effects of velocity and thermal slip conditions have not been taken into account for Maxwell fluid. Such effects are very important for non-Newtonian Maxwell fluids like polymer melts-which exhibit wall slip. Hence, in the present paper, combined effects of viscous dissipation, Joule heating and chemical reaction on the boundary layer flow with velocity and thermal slip is investigated. To the best of the author's knowledge, the problem has not been previously studied. The governing coupled differential equations are solved numerically and all physical characteristics of flow, heat and mass transfer are discussed through graphs and tables. The knowledge will be useful for engineers and scientists when they are interested to boost the efficiency of an upper convected Maxwell fluid flow during industrial processes.

2 Problem Formulation

A two-dimensional steady and incompressible boundary layer flow of an upper-convected chemically reactive Maxwell fluid over a stretching sheet with surface temperature T_w and species concentration C_w is considered. The stretching velocity of the sheet is $U_w(x) = ax$ with a being a constant. The flow is presumed to be generated by stretching sheet issuing from a thin slit at the origin. The sheet is then stretched in such a way that the speed at any point on the sheet becomes proportional to the distance from the origin. Let the wall constant mass transfer be V_w with $V_w > 0$ for injection and $V_w < 0$ for suction. The free stream temperature and species concentration are T_∞ and C_∞ respectively. The coordinate system x - axis is along the stretching sheet while y - axis is normal to the sheet. The flow is subjected to a transverse and uniform magnetic field of strength B_0 which is applied in the positive y - direction, normal to the surface. The magnetic Reynolds number is taken to be small enough so that the induced magnetic field can be neglected. The viscous dissipation and Joule heating are taken into account. Based on these assumptions and following Hayat and Sajid [51] and Sadeghy et al. [52], the governing equations of the conservation of mass, momentum, energy and species concentration, using an order magnitude analysis of the y-direction momentum equation (normal to the sheet) and the usual boundary layer assumptions with negligible pressure gradient where other thermophysical properties remain constant in the presence of magnetic field, past a stretching sheet can be expressed as follows:

$$\frac{\partial u}{\partial x} + \frac{\partial v}{\partial y} = 0 \tag{1}$$

$$u\frac{\partial u}{\partial x} + v\frac{\partial u}{\partial y} + \beta_0\left[v^2\frac{\partial^2 u}{\partial y^2} + 2uv\frac{\partial^2 u}{\partial x \partial y} + u^2\frac{\partial^2 u}{\partial x^2}\right] = \upsilon\frac{\partial^2 u}{\partial y^2} - \frac{\sigma\beta_0^2 u}{\rho} \tag{2}$$

$$\rho C_p\left(u\frac{\partial T}{\partial x} + v\frac{\partial T}{\partial y}\right) = \kappa\frac{\partial^2 T}{\partial y^2} + \mu\left(\frac{\partial u}{\partial u}\right)^2 + \sigma B_0^2 u^2 \tag{3}$$

$$u\frac{\partial C}{\partial x}+v\frac{\partial C}{\partial y}=D_m\frac{\partial^2 C}{\partial y^2}-k_1\left(C-C_\infty\right) \tag{4}$$

where x, y, u, v, T, C, υ, β_0, σ, B_0, ρ, C_p, κ, μ, D_m and k_1 are coordinate axes along the continuous surface in the direction of motion and normal to it, velocity components in the directions of x and y axes, fluid temperature inside the boundary layer, species concentration of the fluid, kinematic viscosity, relaxation time, electrical conductivity, magnetic field strength, fluid density, specific heat at constant pressure, thermal conductivity, dynamic viscosity, mass diffusivity and rate of chemical reaction respectively.

The boundary conditions for the problem are:

$$u=u_w+A\left(\frac{\partial u}{\partial y}\right),\qquad v=V_w, T=T_w+B\frac{\partial T}{\partial y},\qquad C=C_w \quad \text{at } y=0 \tag{5}$$

$$u\to U_\infty=0,\qquad T\to T_\infty,\qquad C\to C_\infty \qquad \text{as} \qquad y\to\infty \tag{6}$$

where $u_w=bx$, $T=T_w+d\left(\frac{x}{l}\right)^2$, l, d, A and B are the reference length of the sheet, a constant, velocity and thermal slip factors respectively. It should be noted that $A=B=0$ corresponds to no-slip condition. The above boundary condition is valid when $x<<l$ which occurs very near to the slit.

Introducing the following dimensionless quantities, the mathematical analysis of the problem is simplified by using the following similarity transforms:

$$\eta=\sqrt{\frac{c}{\upsilon}}y,\quad \psi=\sqrt{c\upsilon}\,x f(\eta),\quad \theta(\eta)=\frac{T-T_\infty}{T_w-T_\infty},\qquad \phi(\eta)=\frac{C-C_\infty}{C_w-C_\infty} \tag{7}$$

The continuity equation (1) is satisfied if a stream function $\psi=(x,y)$ is chosen as:

$$u=\frac{\partial\psi}{\partial y},\qquad v=-\frac{\partial\psi}{\partial x} \tag{8}$$

Using the above similarity transformation quantities, the governing equations (2)-(4) are transformed to the following coupled nonlinear ordinary differential equations:

$$f'''+ff''-\left(f'+Ha\right)f'+\beta\left[2ff'f''-f^2f'''\right]=0 \tag{9}$$

$$\theta''+\Pr Ec\left(f''^2+Haf'^2\right)+\Pr f\,\theta'=0 \tag{10}$$

$$\phi''+Sc\,f\,\phi'-Sc\,Kr\,\phi=0 \tag{11}$$

with boundary conditions:

$$f(0)=R,\ f'(0)=\alpha+\delta f''(0),\ \theta(0)=1+\lambda\theta'(0),\ \phi(0)=1 \text{ at } \eta=0 \tag{12}$$

$$f'(\infty)\to 0,\ \theta(\infty)\to 0,\ \phi(\infty)\to 0 \quad \text{as } \eta\to\infty \tag{13}$$

where the parameters are defined as:

$\beta=\beta_0 a$ is the Deborah number, η is the similarity variable, prime is the differentiation with respect to η, f', θ and ϕ are the dimensionless velocity, temperature and species concentration respectively, $Ha=\dfrac{\sigma\beta_0^2}{c\rho}$ is the magnetic interaction parameter, $\Pr=\dfrac{\mu C_p}{\kappa}$ is the Prandtl number, $Sc=\dfrac{\upsilon}{D_m}$ is the Schmidt number, $R=\dfrac{-V_w}{\sqrt{c\upsilon}}$ is the suction parameter, $\alpha=\dfrac{a}{c}$ is the stretching parameter, $\delta=A\left(\dfrac{c}{\upsilon}\right)^{\frac{1}{2}}$ is the velocity slip parameter, $\lambda=B\left(\dfrac{c}{\upsilon}\right)^{\frac{1}{2}}$ is the thermal slip parameter and $Ec=\dfrac{U_w}{C_p\left(T_w-T_\infty\right)}$ is the Eckert number.

For practical purposes, the functions $f(\eta)$, $\theta(\eta)$ and $\phi(\eta)$ allow for the determination of the skin friction coefficient C_f, Nusselt number Nu_x and Sherwood number Sh_x respectively and they are defined as follows:

$$C_f=\frac{(1+\beta)f''(0)}{\mathrm{Re}_x^{1/2}},\qquad Nu_x=-\mathrm{Re}_x^{1/2}\,\theta'(0),\qquad Sh_x=-\mathrm{Re}_x^{1/2}\,\phi'(0) \tag{14}$$

where $\mathrm{Re}_x=\dfrac{xU_w(x)}{\upsilon}$ is the local Reynolds number.

3 Numerical Solutions

Numerical solutions are obtained for the governing differential equations arising from the problem. An efficient fourth-fifth order Runge-Kutta-Fehlberg method alongside the shooting technique has been employed to investigate the flow model for the above coupled nonlinear ordinary differential equations (9) - (11) with mixed boundary conditions in equations (12) and (13) for different values of embedded governing parameters, namely: Deborah Number β, Hartmann number Ha, Prandtl number $\Pr$, Schmidt number Sc, velocity slip parameter δ, thermal slip parameter λ, Eckert number Ec and rate of chemical reaction parameter Kr. The nonlinear differential equations (9) – (11) are first decomposed into a system of first order differential equations. The coupled ordinary differential equations (9) - (11) are third order in $f(\eta)$ and second order in $\theta(\eta)$ and $\phi(\eta)$ which have been reduced to a system of seven simultaneous equations for seven unknowns. To numerically solve this system of equations using Runge-Kutta-Fehlberg method, the solutions require seven initial boundary conditions in all but two initial conditions in $f(\eta)$, one initial condition in each $\theta(\eta)$ and $\phi(\eta)$ are available. However, the values of $f'(\eta)$, $\theta(\eta)$ and $\phi(\eta)$ are known at $\eta\to\infty$. These free stream conditions are utilized to produce unknown initial conditions at $\eta=0$ by employing shooting technique. The most important of this algorithm is to choose the appropriate finite value of η_∞. Therefore, in order to estimate the value of η_∞, some initial guess values are started

with and the boundary problems consisting of equations (9) - (11) are solved to obtain $f''(0)$, $\theta'(0)$ and $\phi'(0)$. The solution is repeated with another larger value of η_∞ until two successive values of $f''(0)$, $\theta'(0)$ and $\phi'(0)$ differ only after the desired significant digit. The last value η_∞ is taken as the finite value of the limit η_∞ for the particular set of physical parameters for determining the velocity, temperature and the species concentration, which are respectively $f'(\eta)$, $\theta(\eta)$ and $\phi(\eta)$ in the boundary layer. Thus, after getting all the initial conditions, this system of simultaneous equations is solved using the fourth-fifth order Runge-Kutta-Fehlberg integration scheme. The value of $\eta_\infty = 10$ has been selected to be appropriate in nearly all cases for the physical parameters governing the flow. Hence, the coupled boundary value problem of third order in $f(\eta)$, second order in $\theta(\eta)$ and $\phi(\eta)$ has been reduced to a system of seven simultaneous equations of first order for seven unknown variables as follow:

The equations (9) – (11) can be expressed as:

$$f''' = \frac{1}{\left(1-\beta f^2\right)}\left[f'^2 - 2\beta f f' f'' + Ha\, f' - f f''\right] \tag{15}$$

$$\theta'' = -\Pr\left[f\theta' + Ec\left(f''^2 + Ha\, f'^2\right)\right] \tag{16}$$

$$\phi'' = Sc\left[Kr\,\phi - f\phi'\right] \tag{17}$$

The following new variables can be defined using the following equations:

$$f_1 = f(\eta)\ , f_2 = f'(\eta), f_3 = f''(\eta),\ f_4 = \theta(\eta),\ f_5 = \theta'(\eta)\ ,\ f_6 = \theta(\eta),\ f_7 = \theta'(\eta) \tag{18}$$

The coupled higher order nonlinear differential equations and the mixed boundary conditions may be transformed to seven equivalent first-order differential equations and the boundary conditions respectively, as follows:

$$\left.\begin{aligned} f_1' &= f_2 \\ f_2' &= f_3 \\ f_3' &= \frac{\left(f_2^2 - 2\beta f_1 f_2 f_3 + Haf_2 - f_1 f_3\right)}{\left(1-\beta f_1^2\right)} \\ f_4^1 &= f_5 \\ f_5^1 &= -\Pr\left[f_1 f_5 + \left(f_3^{\,2} + Ha\, f_2^{\,2}\right)\right] \\ f_6^1 &= f_7 \\ f_7^1 &= -Sc\left(Kr\, f_6 - f_1 f_7\right) \end{aligned}\right\} \tag{19}$$

Also, the boundary conditions are transformed as:

$$\left.\begin{aligned} &f_1(0) = S,\ f_2(0) = \alpha + \delta f_3(0),\ f_4(0) = 1 + \lambda f_5(0),\ f_6(0) = 1 \\ &f_2(\infty) = 0,\ f_4(\infty) = 0,\ f_6(\infty) = 0 \end{aligned}\right\} \tag{20}$$

Hence, the boundary value problem in equations (9) – (11) with the boundary conditions (12) and (13) is now converted into an initial value problem in equation (19) with the initial conditions in equation (20). Then, the initial value problem is solved by employing Runge-Kutta-Fehlberg integrating scheme appropriately guessing the missing initial values using the shooting method. For several sets of emerging parameters, the step size of $\Delta\eta = 0.001$ is used for the computational purposes by translating the algorithm into MAPLE code as described by Heck [53] and error tolerance of 10^{-7} is used in all the cases. The results obtained are presented through plots for velocity, temperature and species concentration fields and through tables for local skin-friction coefficient, Nusselt and Sherwood numbers.

4 Results and Discussion

This section describes the numerical results obtained. In order to validate the method of solution used in this study and to check the accuracy of the present analysis, a comparison of the present results which correspond to the Nusselt number $\left[-\theta'(0)\right]$ in the absence of thermal and velocity slip effects without consideration for species concentration in a hydrodynamic flow, with the available published results of Hayat et al. [54] for various values of $\Pr$ and α is made and presented in Table 1. This shows a favourable agreement and thus gives confidence that the numerical results obtained are accurate. Tables 2 and 3 depict variations of local skin friction coefficient, Nusselt and Sherwood numbers in relation to β, Ha, R, α, δ, λ, $\Pr$, Ec, Sc and Kr. From these tables, as the values of Deborah number, suction parameter, thermal slip parameter $(\lambda \geq 1)$, stretching parameter, Hartmann, Prandtl and Eckert numbers increase, the values of local skin friction coefficient increase. However, the local skin friction coefficient is found to decrease as the values of velocity slip, thermal slip parameter $(\lambda < 1)$, Schmidt number and rate of chemical reaction parameter increase. Also, it is worth mentioning to note that as the values of $\Pr$, R, α and Ec increase, the local rate of heat transfer (Nusselt number) increases whereas an increase in the values of β, Ha, δ, λ, Sc and Kr is found to decrease the local heat transfer rate. Finally, it is evident from these tables that the local rate of mass transfer is enhanced by increasing the values of Schmidt number, rate of chemical reaction, suction parameter, stretching parameter, thermal slip parameter $(\lambda \geq 1)$, Eckert and Prandtl numbers. Finally, as the values of Hartmann number, Deborah number, thermal slip parameter $(\lambda < 1)$ and velocity slip parameter increase, the local Sherwood number decreases.

Table 1. Comparison of the values of local Nusselt number $-\theta'(0)$ for parameters $\Pr$ and α when $S = 0.5$, $\beta = 0.2$, $Ha = \delta = \phi = Sc = Kr = 0$ with convective boundary conditions

Pr	α	$Nu/\mathrm{Re}_x^{1/2}$ Hayat *et al.* (2011)	$Nu/\mathrm{Re}_x^{1/2}$ (Present Work)
0.5		0.23336	0.23389
1.0		0.36588	0.36625
1.5		0.45796	0.45797
2.0		0.52558	0.52557
1.0	0.1	0.36588	0.36605
	0.3	0.40466	0.40473
	0.8	0.45825	0.45830
	1.0	0.47254	0.47256

Table 2. Values of local skin friction coefficient, Nusselt and Sherwood numbers when $\beta = 0.1$, $\alpha = 0.4$, $Ha = 5$, $R = 0.5$, $\delta = 0.3$, $\lambda = 0.5$, $Ec = 0.5$, $\Pr = 6.7$:

β	Ha	R	α	δ	$-f''(0)$	$-\theta'(0)$	$-\phi'(0)$
0					0.447486483801027	1.94456215130114	1.64438082457562
0.05					0.449240488467801	1.94392969442737	1.64421217986682
0.1					0.451011390964893	1.94327414815704	1.64404259611853
	3				0.409451384781986	1.98214998039128	1.64819171473804
	5				0.451011390964893	1.94327414815704	1.64404259611853
	7				0.479214705390954	1.91690553476665	1.64143871159130
		0.4			0.445564985479499	1.79984582107325	1.58993672262964
		0.6			0.456703499227277	2.06260101728350	1.69962807601467
		0.8			0.468885390452887	2.24891558948133	1.81511702654190
			0.4		0.451011390964893	1.94327414815704	1.64404259611853
			0.5		0.564917738823282	1.99142827253405	1.64842917578333
			0.6		0.679271374624906	2.03266653991193	1.65277945489307
				0.1	0.831653085113820	2.07745831546382	1.65849536970755
				0.3	0.584127108301736	1.99883801287969	1.64916365575298
				0.4	0.508924842474750	1.96867458347552	1.64627960101148

Table 3. Values of local skin friction coefficient, Nusselt and Sherwood numbers when $\beta = 0.1$, $\alpha = 0.4$, $Ha = 5$, $R = 0.5$, $\delta = 0.3$, $\lambda = 0.5$, $Ec = 0.5$, $\Pr = 6.7$:

λ	Pr	Ec	Sc	Kr	$-f''(0)$	$-\theta'(0)$	$-\phi'(0)$
0.6					0.451011390967649	1.28274564507684	1.64404259612261
0.9					0.451011390965383	0.95734077593939	1.64404259612012
1.0					0.451011390969131	0.88270012294364	1.64404259612454
1.3					0.451011390975957	0.71537414632356	1.64404259613243
	1				0.451011390721843	0.53889975623944	1.64404259581782
	5				0.451011390963881	1.67567628007315	1.64404259611777
	7				0.451011390968002	1.98343208121090	1.64404259612241
		0			0.451011390970651	1.71644447685390	1.64404259612604
		0.1			0.451011390970931	1.76181041119071	1.64404259612635
		0.2			0.451011390972202	1.80717634557115	1.64404259612788
			0.5		0.451011390965551	1.94327414819739	1.14347742909375
			1.0		0.451011390965231	1.94327414817597	1.70497039639558
			1.5		0.451011390961850	1.94327414797423	2.17311755488735
				1	0.451011390965952	1.94327414821971	1.25483018279522
				2	0.451011390964893	1.94327414815704	1.64404259611853
				3	0.451011390963642	1.94327414808301	1.94631395911845

Furthermore, the numerical solutions are obtained for the velocity, temperature and species concentration distributions for different values of governing parameters. The results are displayed through graphs in Figs 1-17. It should be pointed out that Figs (1) - (5) satisfy the specified boundary conditions and Figs (6) - (17) unravel the fact that the far field boundary conditions are satisfied asymptotically and hence this also supports the accuracy of the numerical computations and results. The velocity distribution f' for different values of suction parameter R, Deborah number β, Hartmann number Ha, stretching parameter α and velocity slip parameter δ are shown in Figs 1-5 respectively. Fig. 1 shows the influence of R on the flow distribution. It is evident from this figure that f' is a decreasing function of R. This corresponds to the fact that suction which is the removal of fluid from the domain via the porous surface can be used to control the dynamics of Maxwell fluid. Thus, suction enhances adherence of the fluid to the surface which in turn

retards the flow. Fig. 2 displays the velocity distribution with respect to the variation in Deborah number β. As the values of β increases, the velocity distribution in the boundary layer decreases. This implies that a decrease in the fluid velocity corresponds to an enhancement of the velocity boundary layer thickness. From the physical view point, when shear stress is eliminated, the fluid will come to rest. This kind of phenomenon is experienced in many polymeric liquids and this cannot be experienced in the viscous fluid model. Higher values of β will produce a retarding force between two adjacent layers in the flow. For this reason, there will be a reduction in the velocity distribution and corresponding associated effect is noticed in the boundary layer thickness.

Fig. 3 expresses the effect Ha on f'. It is obvious that an increase in the values of Ha decreases the boundary layer thickness in the flow field. Physically, this implies that the magnetic field together with velocity slip effect acts as a controlling force. This force can control the fluid's velocity which is useful in numerous applications such as magnetohydrodynamic power generation and electromagnetic coating of wires and metal. Figs 4 and 5 reveal the distinction of velocity distribution with respect to the variation in velocity slip parameter δ and thermal slip parameter λ. On observing these figures, as the values of both δ and λ increase, the velocity distribution in the boundary layer increases and consequently, the slip parameters decrease the velocity boundary thicknesses as anticipated. Since there is a difference between the average velocities of fluid mixtures in the non-Newtonian Maxwell fluid flowing on a surface and for the fact that in vertical ascending flow, the lighter fluid flows faster than the heavier fluid, the velocity slip therefore depends mainly on the difference in densities of fluids in the different part of the fluid mixtures and their holdups. Considering the thermal slip condition as a result of temperature differences in the region, these result into low fluid densities in the fluid mixtures. Hence, the velocity distribution is enhanced for both velocity and thermal slip parameters.

Figs 6 - 11 illustrate the variations of the dimensionless temperature θ with respect to η for various values of R, Ha, α, $\Pr$, λ and Ec respectively. From Figs 6 and 7, it is observed that R and Ha have opposite effects on θ. An increase in R corresponds to a decrement in the fluid temperature whereas the result of increasing Ha enhances the thermal boundary layer thickness in the flow field. The thermal boundary layers also decrease as the values of α and $\Pr$ increase as displayed in Figs 8 and 9. Higher estimation of $\Pr$ is found to decay the temperature distribution. This is due to the fact that $\Pr$ expresses the ratio of momentum diffusivity to thermal diffusivity. Thus, small values of $\Pr$ implies that the thermal diffusivity dominates and for higher estimation of $\Pr$, the momentum diffusivity dominates. As the values of thermal slip parameter λ increases, the temperature distribution in the flow field increases as shown in Fig. 10 and consequently, the thermal boundary layer thickness and the surface temperature also increase. Fig. 11 demonstrates the variation of dimensionless temperature with the Eckert number Ec which expresses the relationship between a flow's kinetic energy and the boundary layer enthalpy difference. Ec is used to characterize heat dissipation and is found to enhance the thermal boundary layer thickness.

Figs 12 - 17 describe the effects of R, β, Ha, α, Sc and Kr on the species concentration distribution. Fig. 12 captures the influence of R on the species concentration distribution. The species concentration boundary layer is decreased by increasing R. Fig. 13 expresses the effect of β on ϕ. As expected, it is observed that for any given value of η, the species concentration becomes increased with an increase in β. The variations of ϕ with different values of Ha and α are indicated by Figs 14 and 15. It is obvious from these figures that the Hartmann number and stretching parameter have the same effect on the species concentration boundary layer. Both of them noticeably decrease the concentration layer thicknesses. In Fig. 16, it is interesting to note that as the values of Sc increases, it decreases the species concentration boundary layer thickness. This springs from the fact that Sc expresses the ratio of the momentum

diffusivity to the mass diffusivity. Higher values of Sc implies that the momentum diffusivity dominates and hence the species concentration boundary layer is reduced. Fig. 17 is plotted to display the influence of Kr on species concentration distribution in the boundary layer. It is observed that increasing the values of Kr corresponds to an increase in the species concentration boundary layer thickness.

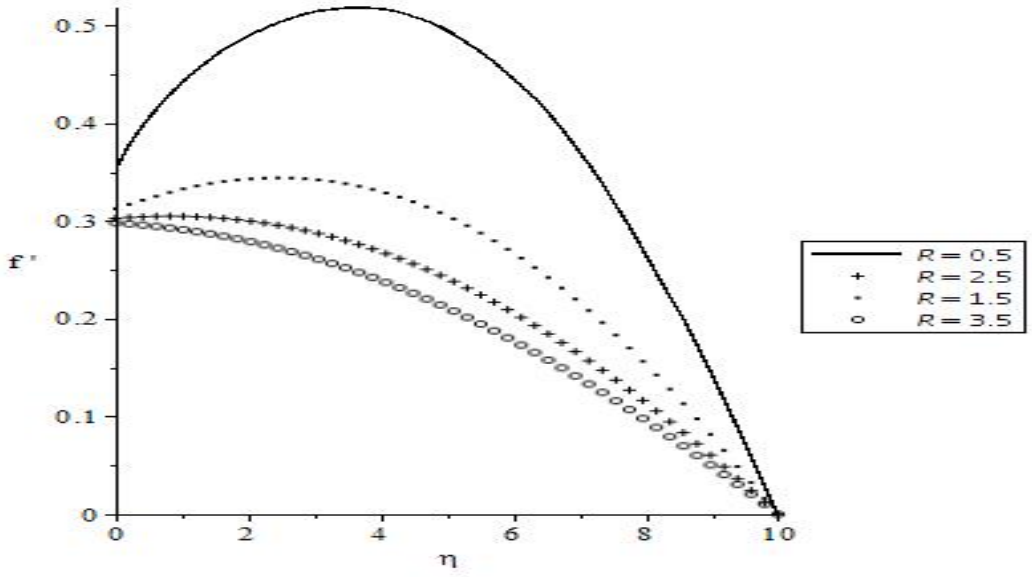

Fig. 1. Velocity distribution for values of R when $Ha = 0.5,\ \beta = 0.5,\ \alpha = 0.3,\ \delta = 0.5$

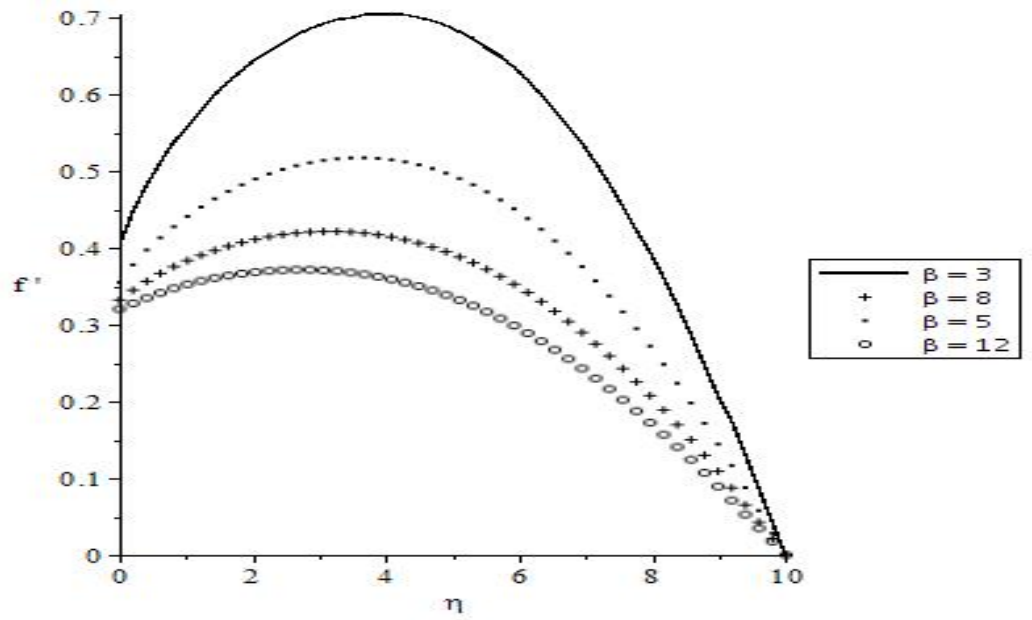

Fig. 2. Velocity distribution for values of β when $Ha = 0.5,\ R = 0.5,\ \alpha = 0.3,\ \delta = 0.5$

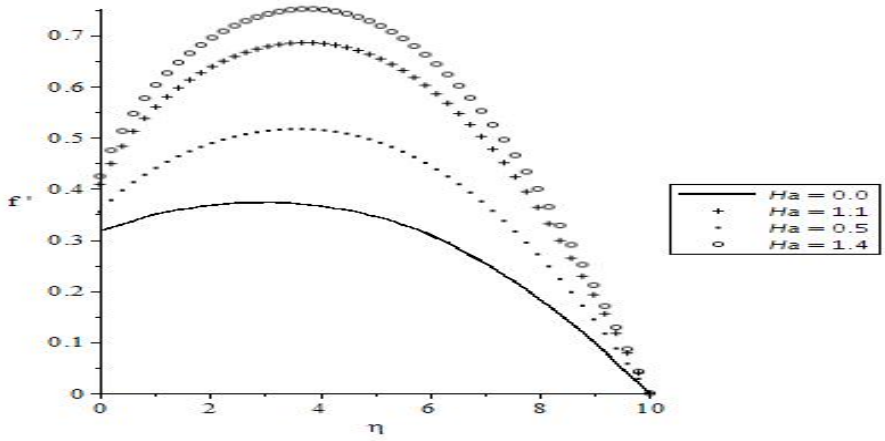

Fig. 3. Velocity distribution for values of Ha when $\beta = 5$, $R = 0.5$, $\alpha = 0.3$, $\delta = 0.5$

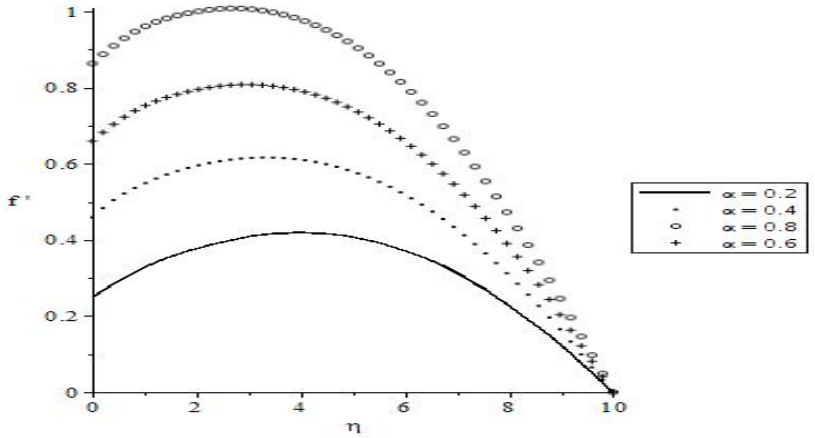

Fig. 4. Velocity distribution for values of α when $Ha = 0.5$, $R = 0.5$, $\beta = 5$, $\delta = 0.5$

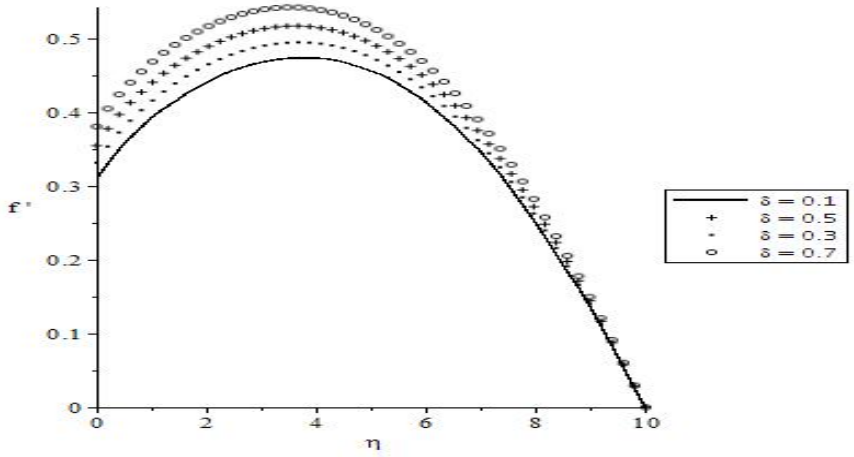

Fig. 5. Velocity distribution for values of δ when $Ha = 0.5$, $R = 0.5$, $\alpha = 0.3$, $\beta = 5$

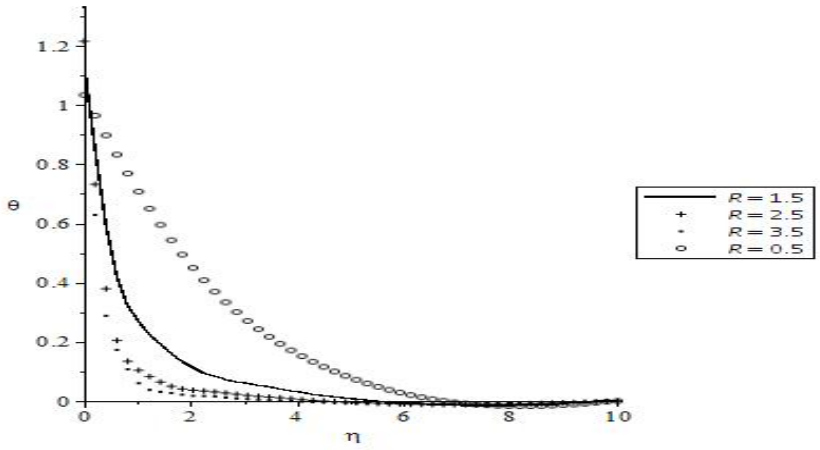

Fig. 6. Temperature distribution for values of R when $Ha = 0.5,\ \Pr = 0.71,\ Ec = 0.1,\ \lambda = 0.1$

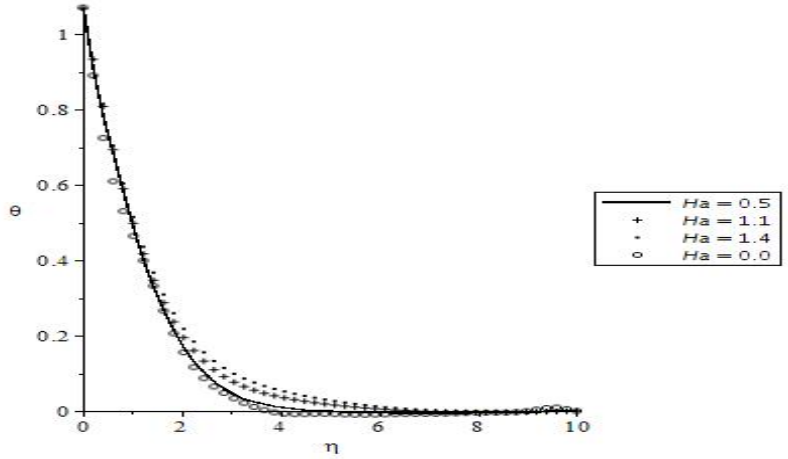

Fig. 7. Temperature distribution for values of Ha when $\Pr = 0.71,\ Ec = 0.1,\ \lambda = 0.1$

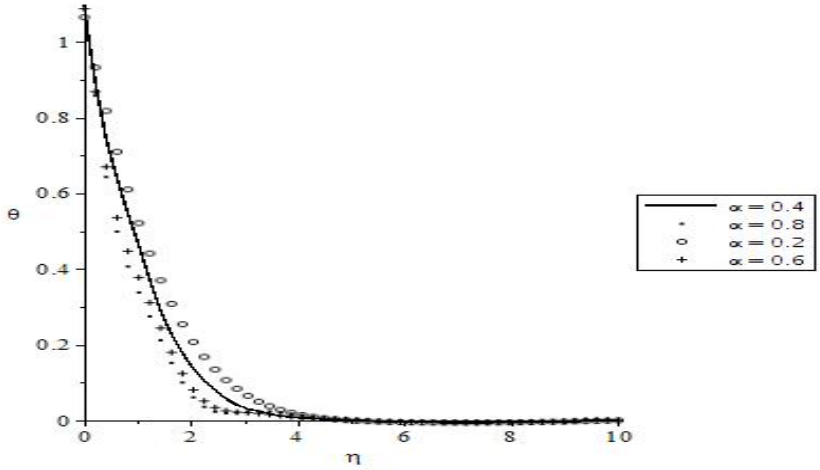

Fig. 8. Temperature distribution for values of α when $\Pr = 0.71,\ Ec = 0.1,\ \lambda = 0.1$

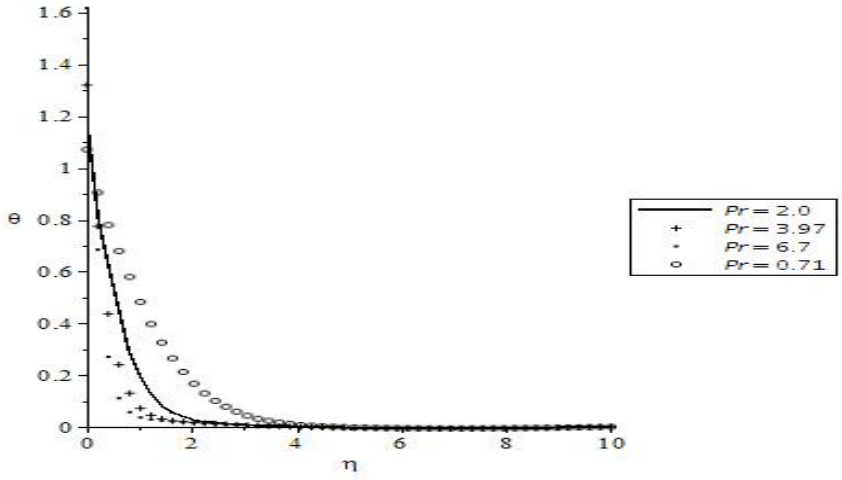

Fig. 9. Temperature distribution for values of $\Pr$ **when** $Ha = 0.5,\ Ec = 0.1,\ \lambda = 0.1$

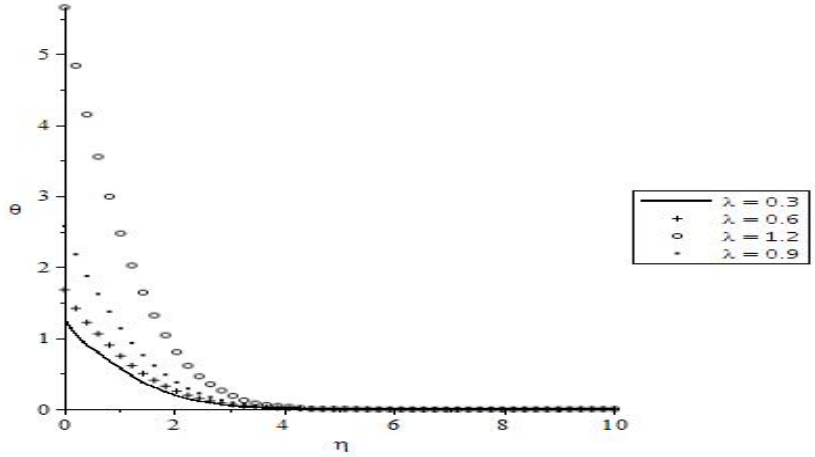

Fig. 10. Temperature distribution for values of λ **when** $Ha = 0.5,\ Ec = 0.1,\ \Pr = 0.71$

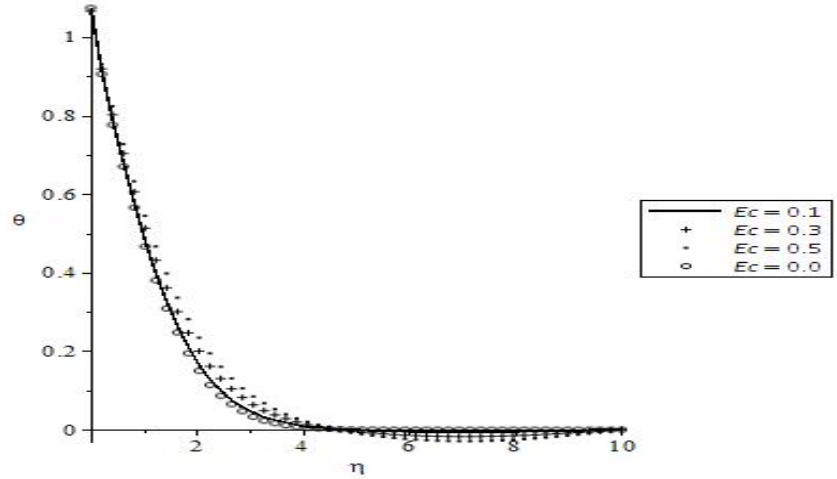

Fig. 11. Temperature distribution for values of Ec **when** $Ha = 0.5,\ \lambda = 0.1,\ \Pr = 0.71$

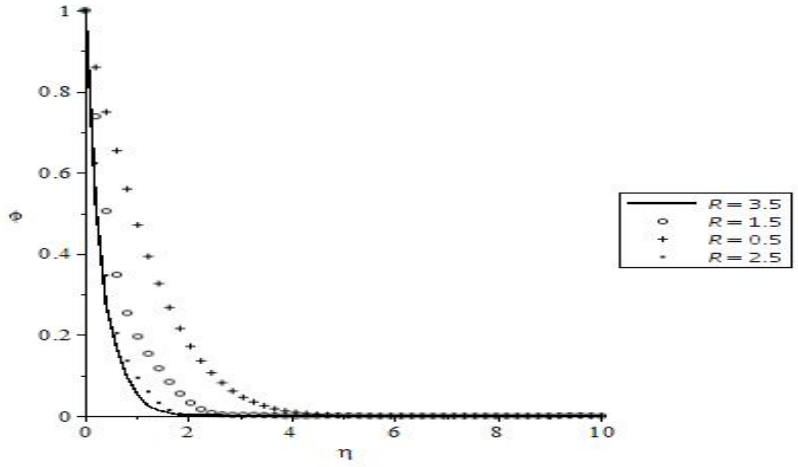

Fig. 12. Species concentration distribution for values of R when $Sc = 0.62$ and $Kr = 1$

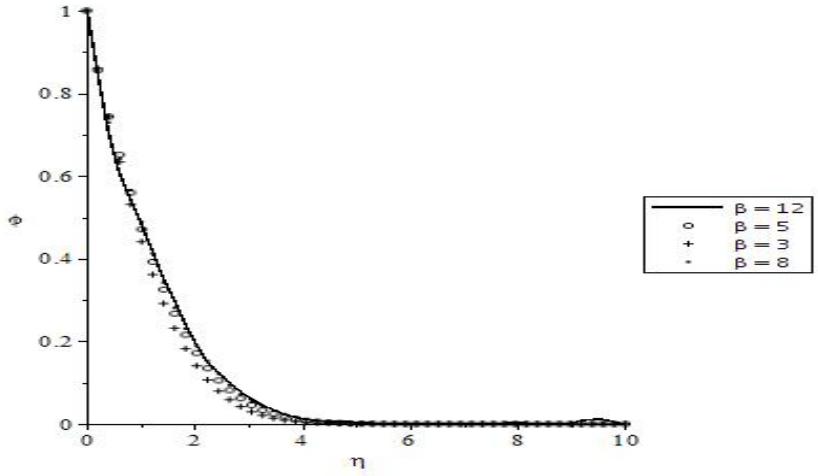

Fig. 13. Species concentration distribution for values of β when $Sc = 0.62$ and $Kr = 1$

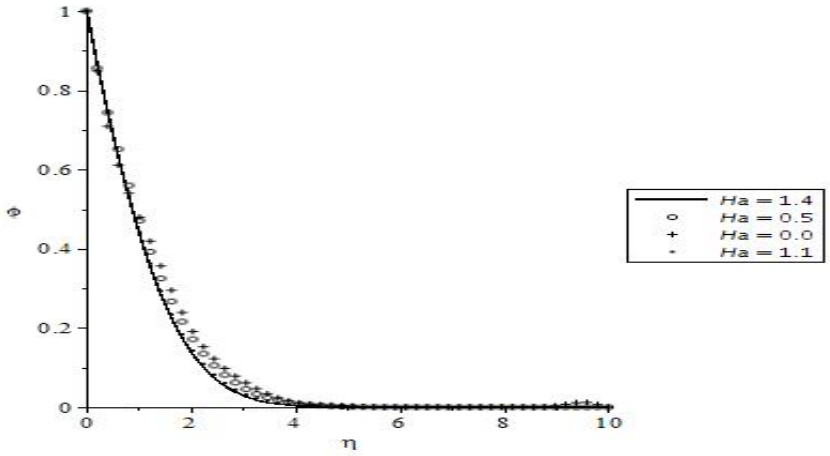

Fig. 14. Species concentration distribution for values of Ha when $Sc = 0.62$ and $Kr = 1$

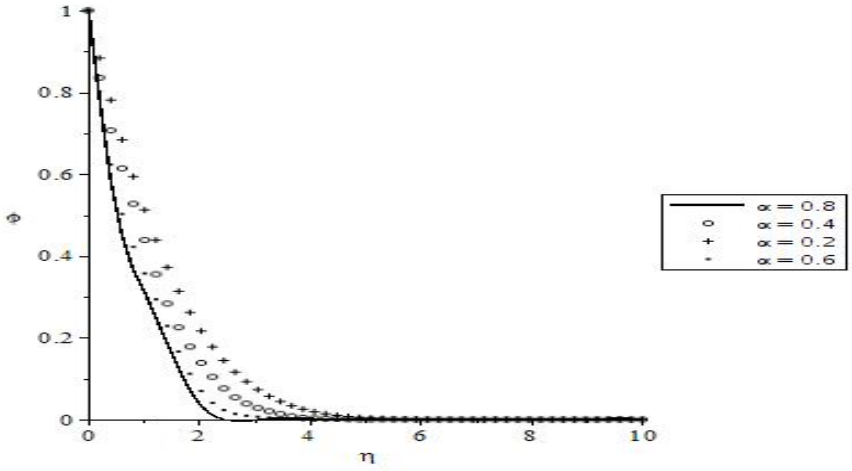

Fig. 15. Species concentration distribution for values of α when $Sc = 0.62$ and $Kr = 1$

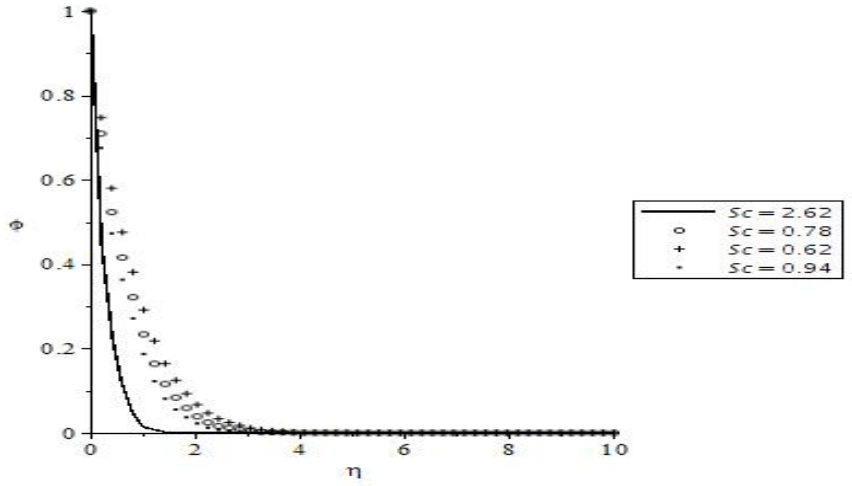

Fig. 16. Species concentration distribution for values of Sc when $Ha = 0.5$ and $Kr = 1$

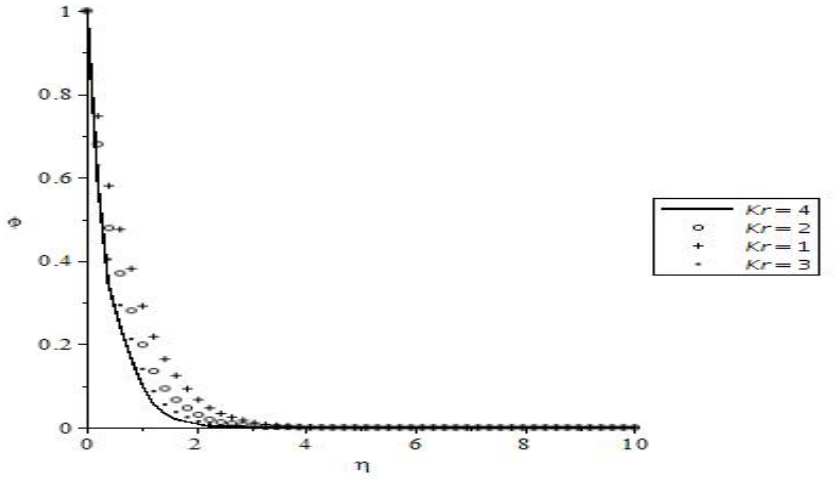

Fig. 17. Species concentration distribution for values of Sc when $Ha = 0.5$ and $Sc = 0.62$

5 Conclusions

In the present investigation, combined influences of viscous dissipation, Joule heating and chemical reaction on an upper-convected Maxwell reactive fluid flow with thermal and velocity slip are examined. Effects of different governing parameters on the velocity, temperature and species concentration are illustrated and discussed. The numerical results give a view towards understanding the characteristics of the flow model of Maxwell fluid on the linearly stretching sheet in the presence of magnetic field, suction and chemical reaction while velocity and thermal slip effects on the flow distribution in the boundary layers are considered. Results for shear stress, rates of thermal and mass transfers at the surface are analyzed and the same are documented in Tables 2 and 3. The numerical solution has been found to be in a very good agreement with the existing analytical results published in the work of Hayat et al. [54] for convective boundary conditions in the absence of species concentration when $Ha = \delta = 0$ as shown in Table 1. The main findings of the study are summarized as follows:

1. It is found that the velocity boundary layer thickness is enhanced by increasing the values of Deborah number, suction and stretching parameters;
2. Thermal boundary layer thickness is increased by increasing values of Hartmann number, Eckert number and thermal slip parameter;
3. Increments in the values of Deborah number and rate of chemical reaction boost the species concentration boundary layer thicknesses;
4. The local skin friction coefficient is reduced by an increase in the values of thermal slip parameter when it is less than unity and velocity slip parameter;
5. Local rates of heat and mass transfer are enhanced by increasing values of suction and stretching parameters.

Competing Interests

Author has declared that no competing interests exist.

References

[1] Crane LJ. Flow past a stretching plate. Z. Angew. Math. Phys. 1970;21:645-647.

[2] Pavlov KB. Magnetohydrodynamic flow of an incompressible viscous fluid caused by the deformation of a plane surface. Magnitnaya Gidrodinamika. 1974;10:146-148.

[3] Gupta, P. S. and, Gupta, A.S. (1977). Heat and mass transfer on a stretching sheet with suction and blowing. Can. J. Chem. Eng. 55, 744-746.

[4] Chen CK, Char MI. Heat transfer of a continuous stretching surface with suction or blowing. J. Math. Anal. Appl. 1988;135:568-580.

[5] Rajagopal, K.R., Na, T.Y. and Gupta, A.S. (1984). Flow of a viscoelastic fluid over a stretching sheet. Rheologica Acta 23, 213-215.

[6] Dandapat BS, Gupta AS. Flow and heat transfer in a viscoelastic fluid over a stretching sheet. International Journal of Nonlinear Mechanics. 1989;24(3):215-219.

[7] Anderson HI. MHD flow of a viscoelastic fluid past a stretching surface. Acta Mechanica. 1992;95:227-230.

[8] Vajravelu K, Nayfeh J. Convective heat transfer at a stretching sheet. Acta Mechanica. 1993;96:47-54.

[9] Eldabe-Nabil TM, Mohammed-Mona AA. Heat and mass transfer in hydromagnetic flow of the non-Newtonian fluid with heat source over an accelerating surface through a porous medium. Chaos Solutions and Fractals. 2002;13:907-917.

[10] Massoudi M, Maneschy CE. Numerical solution to the flow of a second grade fluid over a stretching sheet using the method of quasi-linearization. Applied Mathematics and Computation. 2004;149:165-173.

[11] Siddheshwar PG, Mahabaleshwar US. Effect of radiation and heat transfer on MHD flow of viscoelastic liquid and heat transfer over stretching sheet. International Journal of Nonlinear Mechanics. 2005;40:807-820.

[12] Khan SK, Sanjayand E. Viscoelastic boundary layer flow and heat transfer over an exponentially stretching sheet. International Journal of Heat and Mass Transfer. 2005;48: 1534-1542.

[13] Cortell R. Flow and heat transfer of an electrically conducting fluid of second grade over a stretching sheet subject to suction and a transverse magnetic field. International Journal of Heat and Mass Transfer. 2006;49:1851-1856.

[14] Sanjayanand E, Khan SK. On heat and mass transfer in a viscoelastic boundary layer flow over an exponentially stretching sheet. International Journal of Thermal Science. 2006;45: 819-828.

[15] Hayat T, Saif S, Abbas Z. The influence of heat transfer in an MHD second grade fluid film over an unsteady stretching sheet. Physics Letter A. 2008;372:5037-5045.

[16] Sajid M, Ahmad T, Hayat T, Ayub M. Unsteady flow and heat transfer of a second grade fluid over stretching sheet. Communication in Nonlinear Science and Numerical Simulation. 2009;14:96-108.

[17] Abbas Z, Wang Y, Hayat T, Oberlack M. Mixed convection in the stagnation point flow of a Maxwell fluid towards a vertical stretching surface. Nonlinear Analysis: Real World Applications. 2010;11:3218-3228.

[18] Hayat T, Mustafa M, Pop I. Heat and mass transfer for Soret and Dufour's effect on mixed convection boundary layer flow over a stretching vertical surface in a porous medium filled with a viscoelastic fluid. Communication in Nonlinear Science and Numerical Simulation. 2010;15:1183-1196.

[19] Baoku IG, Onifade YS, Adebayo LO, Yusuff KM. Heat and mass transfer in a second grade fluid over a stretching vertical surface in a porous medium. International Journal of Applied Mechanics and Engineering. 2015;20(2):239-255.

[20] Popoola AA, Baoku IG, Olajuwon BI. Heat and mass transfer on MHD viscoelastic fluid flow in the presence of thermal diffusion and chemical reaction. Journal of Heat and Technology. 2016;34:15-26.

[21] Abd El-Aziz M. Dual solutions in hydromagnetic stagnation point flow and heat transfer towards a stretching/shrinking sheet with non-uniform heat source/sink and variable surface heat flux. Journal of the Egyptian Mathematical Society. 2016;24(3):479-486.

[22] Raza J, Mohd Rohni A, Omar Z. Multiple solutions of mixed convective MHD casson fluid flow in a channel. Journal of Applied Mathematics; 2016.
Available:http://dx.doi.org/10.1155/2016/7535793

[23] Raza J, Mohd Rohni A, Omar Z. Rheology of micropolar fluid in a channel with changing walls: Investigation of multiple solutions. Journal of Molecular Liquids. 2016;223:890-902.
Available:https://doi.org/10.1016/j.molliq.2016.07.102

[24] Raza J, Mohd Rohni A, Omar Z. Triple solutions of Casson fluid flow between slowly expanding and contracting walls. AIP Conference Proceedings. 2017;1905:030029.
Available:https://doi.org/10.1063/1.5012175

[25] Raza J, Mohd Rohni A Omar Z. Unsteady flow of a Casson fluid between two orthogonally moving porous disks: A numerical investigation. Communications in Numerical Analysis. 2017;2:109-124.
DOI: 10.5899/2017/cna-00291

[26] Devakar M, Raje A. A study on the unsteady flow of two immiscible micropolar and Newtonian fluids through a horizontal channel: A numerical approach. The European Physical Journal Plus. 2018;133:180.
Available:https://doi.org/10.1140/epjp/i2018-12011-5

[27] El-Amin MF. Combined effect of viscous dissipation and Joule heating on MHD forced convection over a non-isothermal horizontal cylinder embedded in a fluid saturated porous medium. Journal of Magnetism and Magnetic Materials. 2003;263(3):337-343.
Available:https://doi.org/10.1016/S0304-8853(03)00109-4

[28] Chen C. Combined effects of Joule heating and viscous dissipation on magnetohydrodynamic flow past a permeable, stretching surface with free convection and radiative heat transfer. J. Heat Transfer. 2010;132(6):064503.
DOI: 10.1115/1.4000946

[29] Palani G, Kim K. Joule heating and viscous dissipation effects on MHD Flow past a semi-infinite inclined plate with variable surface temperature. Journal of Engineering Thermophysics. 2011;20(4): 501–517.
DOI: 10.1134/S1810232811040138

[30] Jaber KK. Effects of viscous dissipation and joule heating on MHD flow of a fluid with variable properties past a stretching vertical plate. European Scientific Journal. 2014;10(33)
[ISSN: 1857 – 7881 (Print) e - ISSN 1857- 7431 383]

[31] Jaber KK. Joule heating and viscous dissipation on effects on MHD flow over a stretching porous sheet subjected to power law heat flux in presence of heat source. Open Journal of Fluid Dynamics. 2016;06(03):156-165.
DOI: 10.4236/ojfd.2016.63013

[32] Baoku IG. Corrigendum: Effects of suction and thermal radiation on heat transfer in a third grade fluid over a vertical plate. Physical Science International Journal. 2016;9(2):1-16.
DOI: 10.9734/PSIJ/2016/8964

[33] Kumar KG, Ramesh GK, Gireesha BJ, Gorla RSR. Characteristics of Joule heating and viscous dissipation on three-dimensional flow of Oldroyd-B nanofluid with thermal radiation. Alexandria Engineering Journal; 2017.
Available:https://doi.org/10.1016/j.aej.2017.06.006

[34] Muhammad T, Hayat T, Shehzad SA, Alsaedi A. Viscous dissipation and Joule heating effects in MHD 3D flow with heat and mass fluxes. Results in Physics. 2018;8:365-371.
Available:https://doi.org/10.1016/j.rinp.2017.12.047

[35] Sajid M, Awais M, Nadeem S, Hayat T. The influence of slip condition on thin film flow of a fourth grade fluid by the homotopy analysis method. Computers and Mathematics with Applications. 2008;56:2019-2026.

[36] Sajid M, Awais M, Hayat T. The influence of slip condition on thin film flow of a fourth grade fluid by the homotopy analysis method. Computers and Mathematics with Applications. 2008;56(8):2019-2026.

[37] Hayat T, Hina S, Hendi AA. Slip effects on the magnetohydrodynamic peristaltic flow of a Maxwell fluid, Z. Naturforsh. 2010;65a:1123-1136.

[38] Baoku IG, Olajuwon BI, Mustapha AO. Heat and mass transfer on a MHD third grade fluid with partial slip flow past an infinite vertical insulated porous plate in a porous medium. International Journal of Heat and Fluid Flow. 2013;40:81-88.

[39] Olajuwon BI, Baoku IG. Hydromagnetic partial slip flow, heat and mass transfer of a viscoelastic third grade fluid embedded in a porous medium, Journal of Nonlinear Studies. 2014;21(3):385-401.

[40] Olajuwon BI, Baoku IG. Numerical study of heat and mass transfer in a transient third grade fluid flow in the presence of heat source, chemical reaction and thermal radiation. Daffodil International University Journal of Science and Technology. 2014;9(2):25-36.

[41] Olajuwon BI, Baoku IG, Agboola AAA. Numerical study of a hydromagnetic partial slip flow, heat and mass transfer of a third grade fluid with the presence of thermal radiation through a porous medium. International Journal of Energy and Technology. 2014;6(19):1-17.

[42] Sajid M, Abbas Z, Ali N, Javed T, Ahmad I. Slip flow of a Maxwell fluid past a stretching sheet. Walailak Journal of Science and Technology. 2014;11(12):1093- 1103.

[43] Raza J. Heat and mass transfer analysis of MHD nanofluid flow in a rotating channel with slip effects. Journal of Molecular Liquids. 2016;219:703-708.
DOI: 10.1016/j.molliq.2016.04.003

[44] Raza J, Mohd Rohni A, Omar Z. Numerical investigation of copper-water nanofluid with different shapes of nanoparticles in a channel with stretching wall: Slip effects. Mathematical and Computational Applications. 2016;21:43-57.
DOI: 10.3390/mca21040043

[45] Lin Y, Guo B. Effect of second-order slip on the flow a fractional Maxwell MHD fluid. Journal of the Association of Arab Universities for Basic and Applied Sciences. 2017;24:232-241.

[46] Ullah I, Shafie S, Khan I. Effect of slip condition and Newtonian on MHD flow of Casson fluid over non-linearly stretching sheet saturated in a porous medium. Journal of King Saud University Sciences. 2017;29(2):250-259.

[47] Hayat T, Hina S, Hendi AA. Slip effects on the magnetohydrodynamic peristaltic flow of a Maxwell fluid. Z. Naturforsh. 2010;65a:1123-1136.

[48] Vieru D, Zafar AA. Some couette flows of a Maxwell fluid with wall slip condition. Applied Mathematics and Information Sciences: An International Journal. 2013;7(1):209-219.

[49] Sajid M, Abbas Z, Ali N, Javed T, Ahmad I. Slip flow of a Maxwell fluid past a stretching sheet. Walailak Journal of Science and Technology. 2014;11(12):1093-1103.

[50] Lin Y, Guo B. Effect of second-order slip on the flow a fractional Maxwell MHD fluid. Journal of the Association of Arab Universities for Basic and Applied Sciences. 2017;24:232-241.

[51] Hayat T, Sajid M. Homotopy analysis of MHD boundary layer flow of an upper convected Maxwell fluid. International Journal of Engineering Science. 2007;45:393-401.

[52] Sadeghy K, Najafi AH, Saffaripour M. Sakiadis flow of an upper- convected Maxwell fluid. International Journal of Non-Linear Mechanics. 2005;40:1220-1228.

[53] Heck A. Introduction to Maple. Third Edition, Springer-Verlag, Germany; 2003.

[54] Hayat T, Shehzad SA, Qasim M, Obaidat S. Steady flow of Maxwell fluid with convective boundary conditions. Z. Naturforsch A. 2011;66a:417-422.

Peer-review history:
The peer review history for this paper can be accessed here (Please copy paste the total link in your browser address bar)
http://www.sciencedomain.org/review-history/25478